

A Gegenbauer Polynomial Solution for the Electromagnetic Scattering by a Subwavelength Circular Aperture in an Infinite Conducting Screen

Marios A. Christou¹ and Anastasis C. Polycarpou^{2, *}

Abstract—In this paper, we use magnetic vector potential formulation, along with equivalence principle and image theory, to solve the electromagnetic scattering of a polarized incident plane wave by a subwavelength circular aperture in a conducting screen. The underlined analytical formulation yields a closed-form solution that is accurate for any angle of incidence or polarization and valid for the near-, intermediate- and far-field regions of observation. The formulation is based on Bouwkamp’s diffraction model that uses dominant quasi-static magnetic current modes to represent the governing magnetic current distribution in the circular aperture for any incident wave. Taylor series expansion was implemented on the free-space Green’s function, and the individual Taylor terms were integrated analytically to produce closed-form expressions for the scattered fields in all regions. In doing so, the Gegenbauer polynomial expansion was applied in order to allow evaluation of the resulting integrals for any observation point in the lower half space. The results obtained from the proposed analytical approach were compared with data generated through a direct application of a numerical integration technique. The comparison illustrates the validity and accuracy of the proposed analytical formulation.

1. INTRODUCTION

Optical microscopy [1] is widely used in science and technology to inspect the surface of a sample material through the use of visible light and a magnification lens. The resolution of this technique though is limited by the operating wavelength of the light source. The invention of near-field scanning optical microscopy (NSOM) [2, 3], on the other hand, allowed for a substantial improvement of the spatial resolution of the sample image, compared to conventional optical microscopy. This technique positions the sample under investigation in the near-field region of the subwavelength aperture. In fact, the spatial resolution of the image is limited by the dimension of the circular aperture and not by the wavelength of the illuminating light, as is the case of conventional optical microscopy. Consequently, it is highly important that analytical methods are formulated for the accurate and quick calculation of the corresponding scattered fields.

Scattering of a polarized electromagnetic wave that is obliquely incident on a subwavelength circular aperture in an infinite conducting ground plane has attracted the interest from many scientists and researchers during the last 80 years. Research on the topic started in the mid 40s with the work on the theory of diffraction by small holes published by Bethe [4]. He was able to derived fictitious charges and magnetic currents in the diffracting hole that satisfy Maxwell’s equations and boundary conditions on the conducting screen. A few years later, Bouwkamp [5, 6] provided corrections for these fictitious sources, which significantly improved the results in the near-field region of the aperture. Using these equivalent currents in the context of the vector potential formulation [7], one may evaluate the corresponding

Received 20 February 2019, Accepted 12 May 2019, Scheduled 14 May 2019

* Corresponding author: Anastasis C. Polycarpou (polycarpou.a@unic.ac.cy).

¹ Department of Mathematics, University of Nicosia, Cyprus. ² Department of Engineering, University of Nicosia, Cyprus.

radiation integrals — either in spatial or spectral domain — in order to obtain the diffracted fields due to an incident plane wave. Based on the Bethe and Bouwkamp equivalent models, there were a number of numerical studies on the scattered fields by a circular aperture [8–10]. The derivation of closed-form expressions, however, allows for quick and computationally efficient evaluation of the scattered fields in the vicinity of the aperture.

Back in the 50s, there were other attempts to evaluate the scattering from circular apertures in an exact way. Miexner and Andrejewski [11] obtained a rigorous solution for the scattering from a perfectly conducting, infinitely thin circular disk. Using Babinet’s principle [12], the obtained solution is directly linked to the scattering from a perfectly conducting, infinitely thin screen with a circular aperture. The solution is written in terms of an infinite series of spherical wave eigenfunctions using oblate or prolate spheroidal coordinates. Flammer in 1953 [13] also solved the same problem using a vector wave solution based on oblate spherical vector wave functions. More recently, Roberts [14] used a similar method to solve the problem of diffraction by a circular aperture in a perfectly conducting layer with finite thickness. The electric and magnetic fields, in the interior of the aperture were expanded in terms of circular waveguides modes.

The scattering problem by a circular aperture, based on the Bethe-Bouwkamp model, was later treated using the spectral domain method implementing Fourier transforms and Hankel transform integrals to express the scattered fields in a more convenient way [15–17]. In all these approaches, the incident plane wave was normal to the aperture, which is a simpler special case of the generic scattering problem. It was only recently that Michalski [18] used an approximate complex-image method to compute those Hankel-transform integrals for the oblique incidence. Other researchers worked with the Kobayashi Potential method [19], which is similar to a spectral-domain method of moments (MoM), that implements characteristic functions that satisfy proper edge and boundary conditions, thus producing faster convergent solutions. Such works are available by Nomura and Katsura [20], and later, by Hongo and Naqvi [21].

Recently, Michalski and Mosig [22, 23] revisited the scattering problem for an oblique incidence, and using the spectral domain method, they derived closed-form expressions for the scattered fields in the near- and far-field zone of the aperture. These expressions are easily coded into a computer program in order to produce accurate and timely results for these two regions of observation. However, for the intermediate-field region, the obtained Hankel-transform integrals were evaluated numerically using a procedure based on a Gaussian quadrature with convergence acceleration by extrapolation.

In subsequent work published by the authors [24], a vector potential formulation was used to express the scattered fields in the three regions of observation in terms of radiation integrals. The free-space Green’s function involved in these radiation integrals was written in terms of a Taylor-series expansion about the center of the aperture. This series expansion created individual terms of the form $1/R^{2\alpha}$, where α is a real number and R is the distance from the source to the observation point. As to the difficulty of evaluating those integrals for any observation angle, the analysis was limited only to computation of the scattered fields along the axis of the aperture. In this work, we use a Gegenbauer polynomial expansion in order to evaluate the radiation integrals in spatial domain and for any angle of observation. This work results in closed-form expressions for the scattered electric fields everywhere in the lower half space of the aperture. The analysis is given only for the case where the radial distance r is larger than the radius of the aperture.

In the following section, Section 2, we present the formulation of the problem based on the electric vector potential. The use of Taylor- and Gegenbauer-series expansions are explained and demonstrated. In Section 3, we present analytical results obtained with the proposed method. For validation purposes, these are compared with numerical results obtained using a numerical integration. Concluding remarks are presented in Section 4.

2. PROBLEM FORMULATION

The formulation of the problem is based on the geometry shown in Fig. 1. A linearly polarized plane wave is incident on a circular aperture in an infinite conducting screen of zero thickness. The origin of the coordinate system coincides with the center of the circular aperture, and the positive z -axis is directed downwards in the lower half space. Due to the rotational symmetry of the problem, we assume

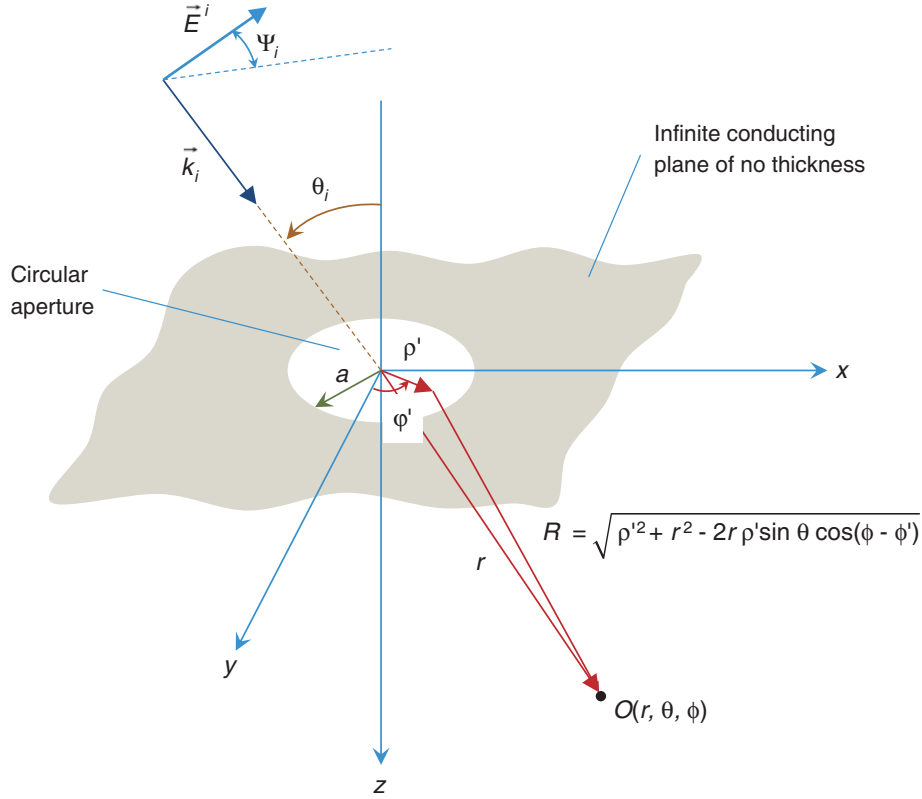


Figure 1. Problem geometry.

that the plane of incidence corresponds to the x - z plane, as shown in the figure. The incident angle, θ_i , is measured between the incident propagation vector, \vec{k}_i , and the positive z -axis. The polarization of the wave is defined by the angle ψ_i , which is measured from the plane of incidence to the electric-field vector. Specifically, for $\psi_i = 0^\circ$, the polarization corresponds to a TM-wave, and for $\psi_i = 90^\circ$, the polarization corresponds to a TE-wave.

An incident plane wave, of arbitrary polarization defined by angle ψ_i , is given by

$$\vec{E}_i = \hat{a}_e e^{-jk(\kappa_{xi}x + \kappa_{zi}z)} \tag{1}$$

where

$$\hat{a}_e = \hat{a}_x \kappa_{zi} \cos \psi_i + \hat{a}_y \sin \psi_i - \hat{a}_z \kappa_{xi} \cos \psi_i \tag{2}$$

$$\kappa_{xi} = \frac{k_{xi}}{k} = \sin \theta_i, \quad \kappa_{zi} = \frac{k_{zi}}{k} = \cos \theta_i \tag{3}$$

The equivalence principle, along with the image theory, can be used to determine the scattered fields in the lower half space provided the magnetic current density distribution is known in the aperture. According to the Bouwkamp diffraction model [5], which provides an improvement over the theory of diffraction by small holes published by Bethe a few years earlier [4], the governing magnetic current density due to an incident plane wave can be approximated by the dominant modes provided that the largest dimension of the aperture is only a fraction of the operating wavelength. As a result, the magnetic current density can be expressed in terms of two orthogonal components:

$$\vec{M} = \hat{a}_\rho M_\rho + \hat{a}_\phi M_\phi \tag{4}$$

where

$$M_\rho = \frac{4jk}{3\pi} [\kappa_{xi}^2 \cos \psi_i \sin \phi' - 2s_i(\phi')] \sqrt{a^2 - \rho'^2} \tag{5}$$

$$M_\phi = \frac{2\kappa_{xi} \cos \psi_i}{\pi} \frac{\rho'}{\sqrt{a^2 - \rho'^2}} + \frac{4jk}{3\pi} \left\{ \kappa_{xi}^2 \cos \psi_i \cos \phi' \frac{a^2 - 2\rho'^2}{\sqrt{a^2 - \rho'^2}} - c_i(\phi') \frac{2a^2 - \rho'^2}{\sqrt{a^2 - \rho'^2}} \right\} \quad (6)$$

and

$$s_i(\phi') = \cos \psi_i \sin \phi' - \kappa_{zi} \sin \psi_i \cos \phi' \quad (7)$$

$$c_i(\phi') = \cos \psi_i \cos \phi' + \kappa_{zi} \sin \psi_i \sin \phi' \quad (8)$$

Note that a is the radius of the aperture, and (ρ', ϕ') corresponds to an arbitrary source point in the circular domain (see Fig. 1). The magnetic vector potential formulation can be used to solve for the scattered fields by the aperture. Specifically, the magnetic vector potential can be expressed as a double integration of the magnetic current density multiplied by the free-space Green's function [7]. Knowing the vector potential \vec{F} , the electric and magnetic fields at an observation point in the lower half space can be expressed as follows:

$$\vec{E} = \vec{E}_F = -\frac{1}{\epsilon} \nabla \times \vec{F} \quad (9)$$

$$\vec{H} = \vec{H}_F = -\frac{1}{j\omega\mu} \nabla \times \vec{E}_F \quad (10)$$

2.1. Derivation of the Scattered Electric Fields

Using basic electromagnetic theory [7], the vector potential \vec{F} can be formulated in terms of a surface integration over the circular aperture. The equivalence principle, along with the image theory, can be implemented in order to simplify the problem for the evaluation of the fields in the lower half space. By taking the curl of the vector potential, according to Eq. (9), the scattered electric field expressions are derived:

$$E_r = -\frac{1}{2\pi} \iint_S M_\phi \cos \theta \rho' \hat{G}_o dS' \quad (11)$$

$$E_\theta = -\frac{r}{2\pi} \iint_S [-M_\rho \sin \xi + M_\phi \cos \xi] \hat{G}_o dS' + \frac{1}{2\pi} \iint_S M_\phi \sin \theta \rho' \hat{G}_o dS' \quad (12)$$

$$E_\phi = \frac{r}{2\pi} \iint_S \cos \theta [M_\rho \cos \xi + M_\phi \sin \xi] \hat{G}_o dS' \quad (13)$$

where

$$\hat{G}_o = \left(\frac{jk}{R^2} + \frac{1}{R^3} \right) e^{-jkR} \quad (14)$$

$$R = \sqrt{\rho'^2 + r^2 - 2r\rho' \sin \theta \cos \xi} \quad (15)$$

$$\xi = \phi - \phi' \quad (16)$$

A Taylor-series expansion about the origin of the coordinate system is introduced for the exponential function e^{-jkR} :

$$e^{-jkR} = 1 - jkR - \frac{k^2 R^2}{2!} + \frac{jk^3 R^3}{3!} + \dots = \sum_{n=0}^{\infty} \frac{(-1)^n (jk)^n}{n!} R^n \quad (17)$$

Substituting Eq. (17) into Eq. (14) and collecting terms according to the integer power of R , the modified Green's function \hat{G}_o becomes

$$\hat{G}_o = \sum_{m=1}^{\infty} C(m) R^{m-4} \quad (18)$$

where

$$C(m) = \frac{(-1)^{m-4} (m-2) (jk)^{m-1}}{(m-1)!} \quad (19)$$

The convergence of the series in Eq. (18) can be shown using the Cauchy’s ratio test, which involves the $m + 1$ and m general terms:

$$u_m = \frac{(-1)^{m-4}(m-2)(jk)^{m-1}}{(m-1)!} R^{m-4}$$

$$u_{m+1} = \frac{(-1)^{m-3}(m-1)(jk)^m}{m!} R^{m-3}$$

The ratio test yields the following result:

$$\lim_{m \rightarrow \infty} \left| \frac{u_{m+1}}{u_m} \right| = |jkR| \lim_{m \rightarrow \infty} \frac{m-1}{m^2-2m} = 0 \tag{20}$$

Absolute convergence is guaranteed because the limit is zero as the index m approaches infinity. Note, however, that the rate of convergence becomes increasingly slower as the observation distance R , measured from the source point, increases.

Starting with the evaluation of the θ -component of the electric field, the latter can be expressed as a superposition of three distinct terms:

$$E_\theta = E_\theta^{(1)} + E_\theta^{(2)} + E_\theta^{(3)} \tag{21}$$

where

$$E_\theta^{(1)} = \frac{r}{2\pi} \sum_{m=1}^{\infty} C(m) \int_0^a \int_0^{2\pi} M_\rho \sin \xi R^{m-4} \rho' d\phi' d\rho' \tag{22}$$

$$E_\theta^{(2)} = -\frac{r}{2\pi} \sum_{m=1}^{\infty} C(m) \int_0^a \int_0^{2\pi} M_\phi \cos \xi R^{m-4} \rho' d\phi' d\rho' \tag{23}$$

$$E_\theta^{(3)} = \frac{\sin \theta}{2\pi} \sum_{m=1}^{\infty} C(m) \int_0^a \int_0^{2\pi} M_\phi R^{m-4} \rho'^2 d\phi' d\rho' \tag{24}$$

Based on the above expressions, let us define the following double integrals:

$$I_\theta^{(1)} = \int_0^a \int_0^{2\pi} M_\rho \sin \xi R^{m-4} \rho' d\phi' d\rho' \tag{25}$$

$$I_\theta^{(2)} = \int_0^a \int_0^{2\pi} M_\phi \cos \xi R^{m-4} \rho' d\phi' d\rho' \tag{26}$$

$$I_\theta^{(3)} = \int_0^a \int_0^{2\pi} M_\phi R^{m-4} \rho'^2 d\phi' d\rho' \tag{27}$$

Each one of these integrals can be further broken down into simpler terms due to the definition of the governing magnetic current densities in the aperture. For example, Eq. (25), can be expressed in the form:

$$I_\theta^{(1)} = I_\theta^{(1,1)} + I_\theta^{(1,2)} + I_\theta^{(1,3)} \tag{28}$$

where

$$I_\theta^{(1,1)} = \frac{4jk}{3\pi} k_{xi}^2 \cos \psi_i \int_0^a \int_0^{2\pi} \sin \phi' F_1(R, \rho') d\phi' d\rho' \tag{29}$$

$$I_{\theta}^{(1,2)} = -\frac{8jk}{3\pi} \cos \psi_i \int_0^a \int_0^{2\pi} \sin \phi' F_1(R, \rho') d\phi' d\rho' \quad (30)$$

$$I_{\theta}^{(1,3)} = \frac{8jk}{3\pi} k_{zi} \sin \psi_i \int_0^a \int_0^{2\pi} \cos \phi' F_1(R, \rho') d\phi' d\rho' \quad (31)$$

and

$$F_1(\xi, R, \rho') = \sin \xi R^{m-4} \rho' \sqrt{a^2 - \rho'^2} \quad (32)$$

Likewise, the second double integral in Eq. (26) can be written in the form:

$$I_{\theta}^{(2)} = I_{\theta}^{(2,1)} + I_{\theta}^{(2,2)} + I_{\theta}^{(2,3)} + I_{\theta}^{(2,4)} \quad (33)$$

where

$$I_{\theta}^{(2,1)} = \frac{2k_{xi} \cos \psi_i}{\pi} \int_0^a \int_0^{2\pi} F_2(\xi, R, \rho') d\phi' d\rho' \quad (34)$$

$$I_{\theta}^{(2,2)} = \frac{4jk}{3\pi} k_{xi}^2 \cos \psi_i \int_0^a \int_0^{2\pi} \cos \phi' F_3(\xi, R, \rho') d\phi' d\rho' \quad (35)$$

$$I_{\theta}^{(2,3)} = -\frac{4jk}{3\pi} \cos \psi_i \int_0^a \int_0^{2\pi} \cos \phi' F_4(\xi, R, \rho') d\phi' d\rho' \quad (36)$$

$$I_{\theta}^{(2,4)} = -\frac{4jk}{3\pi} k_{zi} \sin \psi_i \int_0^a \int_0^{2\pi} \sin \phi' F_4(\xi, R, \rho') d\phi' d\rho' \quad (37)$$

and

$$F_2(\xi, R, \rho') = \cos \xi R^{m-4} \frac{\rho'^2}{\sqrt{a^2 - \rho'^2}} \quad (38)$$

$$F_3(\xi, R, \rho') = \cos \xi R^{m-4} \frac{a^2 - 2\rho'^2}{\sqrt{a^2 - \rho'^2}} \quad (39)$$

$$F_4(\xi, R, \rho') = \cos \xi R^{m-4} \frac{2a^2 - \rho'^2}{\sqrt{a^2 - \rho'^2}} \quad (40)$$

For the last integral in Eq. (27), we can write

$$I_{\theta}^{(3)} = I_{\theta}^{(3,1)} + I_{\theta}^{(3,2)} + I_{\theta}^{(3,3)} + I_{\theta}^{(3,4)} \quad (41)$$

where

$$I_{\theta}^{(3,1)} = \frac{2k_{xi} \cos \psi_i}{\pi} \int_0^a \int_0^{2\pi} F_5(R, \rho') d\phi' d\rho' \quad (42)$$

$$I_{\theta}^{(3,2)} = \frac{4jk}{3\pi} k_{xi}^2 \cos \psi_i \int_0^a \int_0^{2\pi} \cos \phi' F_6(R, \rho') d\phi' d\rho' \quad (43)$$

$$I_{\theta}^{(3,3)} = -\frac{4jk}{3\pi} \cos \psi_i \int_0^a \int_0^{2\pi} \cos \phi' F_7(R, \rho') d\phi' d\rho' \quad (44)$$

$$I_{\theta}^{(3,4)} = -\frac{4jk}{3\pi} k_{zi} \sin \psi_i \int_0^a \int_0^{2\pi} \sin \phi' F_7(R, \rho') d\phi' d\rho' \tag{45}$$

and

$$F_5(R, \rho') = \rho' R^{m-4} \frac{\rho'^2}{\sqrt{a^2 - \rho'^2}} \tag{46}$$

$$F_6(R, \rho') = \rho' R^{m-4} \frac{a^2 - 2\rho'^2}{\sqrt{a^2 - \rho'^2}} \tag{47}$$

$$F_7(R, \rho') = \rho' R^{m-4} \frac{2a^2 - \rho'^2}{\sqrt{a^2 - \rho'^2}} \tag{48}$$

Concerning the radial component of the electric field, the governing expression is very similar to the expression for $I_{\theta}^{(3)}$. As a result, the E_r component can be conveniently written as

$$E_r = -\frac{r \cos \theta}{2\pi} \sum_{m=1}^{\infty} C(m) I_{\theta}^{(3)}, \quad \theta \in [0, 2\pi] \tag{49}$$

The third component of the electric field, E_{ϕ} , can be expressed in the following form:

$$E_{\phi} = E_{\phi}^{(1)} + E_{\phi}^{(2)} \tag{50}$$

where

$$E_{\phi}^{(1)} = \frac{r \cos \theta}{2\pi} \sum_{m=1}^{\infty} C(m) \int_0^a \int_0^{2\pi} M_{\rho} \cos \xi R^{m-4} \rho' d\phi' d\rho' \tag{51}$$

$$E_{\phi}^{(2)} = \frac{r \cos \theta}{2\pi} \sum_{m=1}^{\infty} C(m) \int_0^a \int_0^{2\pi} M_{\phi} \sin \xi R^{m-4} \rho' d\phi' d\rho' \tag{52}$$

Based on the aforementioned expressions, we can define the following two integrals:

$$I_{\phi}^{(1)} = \int_0^a \int_0^{2\pi} M_{\rho} \cos \xi R^{m-4} \rho' d\phi' d\rho' \tag{53}$$

$$I_{\phi}^{(2)} = \int_0^a \int_0^{2\pi} M_{\phi} \sin \xi R^{m-4} \rho' d\phi' d\rho' \tag{54}$$

The first integral in Eq. (53) can be broken down into three individual terms:

$$I_{\phi}^{(1)} = I_{\phi}^{(1,1)} + I_{\phi}^{(1,2)} + I_{\phi}^{(1,3)} \tag{55}$$

where

$$I_{\phi}^{(1,1)} = \frac{4jk}{3\pi} k_{xi}^2 \cos \psi_i \int_0^a \int_0^{2\pi} \sin \phi' F_8(R, \rho') d\phi' d\rho' \tag{56}$$

$$I_{\phi}^{(1,2)} = -\frac{8jk}{3\pi} \cos \psi_i \int_0^a \int_0^{2\pi} \sin \phi' F_8(R, \rho') d\phi' d\rho' \tag{57}$$

$$I_{\phi}^{(1,3)} = \frac{8jk}{3\pi} k_{zi} \sin \psi_i \int_0^a \int_0^{2\pi} \cos \phi' F_8(R, \rho') d\phi' d\rho' \tag{58}$$

and

$$F_8(\xi, R, \rho') = \cos \xi R^{m-4} \rho' \sqrt{a^2 - \rho'^2} \quad (59)$$

The second double integral in Eq. (54) can be broken down into four terms:

$$I_\phi^{(2)} = I_\phi^{(2,1)} + I_\phi^{(2,2)} + I_\phi^{(2,3)} + I_\phi^{(2,4)} \quad (60)$$

where

$$I_\phi^{(2,1)} = \frac{2k_{xi} \cos \psi_i}{\pi} \int_0^a \int_0^{2\pi} F_9(\xi, R, \rho') d\phi' d\rho' \quad (61)$$

$$I_\phi^{(2,2)} = \frac{4jk}{3\pi} k_{xi}^2 \cos \psi_i \int_0^a \int_0^{2\pi} \cos \phi' F_{10}(\xi, R, \rho') d\phi' d\rho' \quad (62)$$

$$I_\phi^{(2,3)} = -\frac{4jk}{3\pi} \cos \psi_i \int_0^a \int_0^{2\pi} \cos \phi' F_{11}(\xi, R, \rho') d\phi' d\rho' \quad (63)$$

$$I_\phi^{(2,4)} = -\frac{4jk}{3\pi} k_{zi} \sin \psi_i \int_0^a \int_0^{2\pi} \sin \phi' F_{11}(\xi, R, \rho') d\phi' d\rho' \quad (64)$$

and

$$F_9(\xi, R, \rho') = \sin \xi R^{m-4} \frac{\rho'^2}{\sqrt{a^2 - \rho'^2}} \quad (65)$$

$$F_{10}(\xi, R, \rho') = \sin \xi R^{m-4} \frac{a^2 - 2\rho'^2}{\sqrt{a^2 - \rho'^2}} \quad (66)$$

$$F_{11}(\xi, R, \rho') = \sin \xi R^{m-4} \frac{2a^2 - \rho'^2}{\sqrt{a^2 - \rho'^2}} \quad (67)$$

The objective now is to evaluate analytically all these double integrals over the domain of the circular aperture. This is achieved through the use of Gegenbauer polynomial expansion which is explained in detail in the following section.

2.2. Analytical Evaluation of the Double Integrals

As shown in the previous subsection, all integrals involved in the evaluation of the scattered fields in the lower half space incorporate the term $1/R^{2\alpha}$, where $\alpha = 4 - m$. Note that R , which is the distance from the source point to the observation point, is dependent not only on the cylindrical coordinates of the source point, but also on the azimuth and elevation angles of the observation point. In an earlier paper by the authors [24], the scattered fields were solved for the special case where the observation point lies on the z -axis; i.e., the angle θ was set equal to zero. In order to facilitate the analytical solution of the scattered fields for off-axis observation, we implement a Gegenbauer polynomial expansion [25] of the $1/R^{2\alpha}$ term:

$$\frac{1}{(r^2 + \rho'^2 - 2r\rho' \sin \theta \cos \xi)^\alpha} = \sum_{n=0}^{\infty} \frac{\rho'^n}{r^{n+2\alpha}} C(\sin \theta \cos \xi) \quad (68)$$

where C is the Gegenbauer polynomial which can be written as a finite sum of gamma functions:

$$C(\sin \theta \cos \xi) = \sum_{k=0}^{\lfloor n/2 \rfloor} (-1)^k \frac{\Gamma(n - k + \alpha)}{\Gamma(\alpha) k! (n - 2k)!} (2 \sin \theta \cos \xi) \quad (69)$$

The Gegenbauer polynomial expansion in Eq. (68) is convergent only for cases where $r > \rho'$. This is guaranteed only for observation points where $r > a$, where a is the radius of the aperture.

Using the series expansion in Eq. (68), the $I_{\theta}^{(1)}$ integrals can be conveniently expressed as follows:

$$I_{\theta}^{(1,1)} = -\frac{4jk}{3\pi} k_{xi}^2 \cos \psi_i \cos \phi S_1 \tag{70}$$

$$I_{\theta}^{(1,2)} = \frac{8jk}{3\pi} \cos \psi_i \cos \phi S_1 \tag{71}$$

$$I_{\theta}^{(1,3)} = \frac{8jk}{3\pi} k_{zi} \sin \psi_i \sin \phi S_1 \tag{72}$$

where

$$S_1 = \sum_{n=0}^{\infty} \sum_{k=0}^{[n/2]} (-1)^k \frac{\Gamma(n-k+\alpha)(2\sin\theta)^{n-2k}}{\Gamma(\alpha)k!(n-2k)!} \cdot \frac{a^{n+3}}{r^{n+2\alpha}} \cdot (K_1(n-2k) - K_1(n-2k+2)) \cdot (K_2(n+1) - K_2(n+3)) \tag{73}$$

and

$$K_1(p) = \int_0^{2\pi} \cos^p w dw, \quad K_2(p) = \int_0^{\pi/2} \sin^p w dw \tag{74}$$

Similarly, the integrals $I_{\theta}^{(2)}$ can be written as

$$I_{\theta}^{(2,1)} = \frac{2k_{xi} \cos \psi_i}{\pi} S_2 \tag{75}$$

$$I_{\theta}^{(2,2)} = \frac{4jk}{3\pi} k_{xi}^2 \cos \psi_i \cos \phi S_3 \tag{76}$$

$$I_{\theta}^{(2,3)} = -\frac{4jk}{3\pi} \cos \psi_i \cos \phi S_4 \tag{77}$$

$$I_{\theta}^{(2,4)} = -\frac{4jk}{3\pi} k_{zi} \sin \psi_i \sin \phi S_4 \tag{78}$$

where

$$S_2 = \sum_{n=0}^{\infty} \sum_{k=0}^{[n/2]} (-1)^k \frac{\Gamma(n-k+\alpha)(2\sin\theta)^{n-2k}}{\Gamma(\alpha)k!(n-2k)!} \cdot \frac{a^{n+2}}{r^{n+2\alpha}} \cdot K_1(n+1-2k) \cdot K_2(n+2) \tag{79}$$

$$S_3 = \sum_{n=0}^{\infty} \sum_{k=0}^{[n/2]} (-1)^k \frac{\Gamma(n-k+\alpha)(2\sin\theta)^{n-2k}}{\Gamma(\alpha)k!(n-2k)!} \cdot \frac{a^{n+3}}{r^{n+2\alpha}} \cdot K_1(n+2-2k) \cdot (K_2(n+1) - 2K_2(n+3)) \tag{80}$$

$$S_4 = \sum_{n=0}^{\infty} \sum_{k=0}^{[n/2]} (-1)^k \frac{\Gamma(n-k+\alpha)(2\sin\theta)^{n-2k}}{\Gamma(\alpha)k!(n-2k)!} \cdot \frac{a^{n+3}}{r^{n+2\alpha}} \cdot K_1(n+2-2k) \cdot (2K_2(n+1) - K_2(n+3)) \tag{81}$$

As far as the integrals $I_{\theta}^{(3)}$ are concerned, the use of the Gegenbauer polynomial expansion yields

$$I_{\theta}^{(3,1)} = \frac{2k_{xi} \sin \theta \cos \psi_i}{\pi} S_5 \tag{82}$$

$$I_{\theta}^{(3,2)} = \frac{4jk}{3\pi} k_{xi}^2 \sin \theta \cos \psi_i \cos \phi S_6 \tag{83}$$

$$I_{\theta}^{(3,3)} = -\frac{4jk}{3\pi} \sin \theta \cos \psi_i \cos \phi S_7 \tag{84}$$

$$I_{\theta}^{(3,4)} = -\frac{4jk}{3\pi} k_{zi} \sin \theta \sin \psi_i \sin \phi S_7 \tag{85}$$

where

$$\mathbb{S}_5 = \sum_{n=0}^{\infty} \sum_{k=0}^{\lfloor n/2 \rfloor} (-1)^k \frac{\Gamma(n-k+\alpha)(2\sin\theta)^{n-2k}}{\Gamma(\alpha)k!(n-2k)!} \cdot \frac{a^{n+3}}{r^{n+2\alpha}} \cdot \mathbf{K}_1(n-2k) \cdot \mathbf{K}_2(n+3) \quad (86)$$

$$\mathbb{S}_6 = \sum_{n=0}^{\infty} \sum_{k=0}^{\lfloor n/2 \rfloor} (-1)^k \frac{\Gamma(n-k+\alpha)(2\sin\theta)^{n-2k}}{\Gamma(\alpha)k!(n-2k)!} \cdot \frac{a^{n+4}}{r^{n+2\alpha}} \cdot \mathbf{K}_1(n+1-2k) \cdot (\mathbf{K}_2(n+2) - 2\mathbf{K}_2(n+4)) \quad (87)$$

$$\mathbb{S}_7 = \sum_{n=0}^{\infty} \sum_{k=0}^{\lfloor n/2 \rfloor} (-1)^k \frac{\Gamma(n-k+\alpha)(2\sin\theta)^{n-2k}}{\Gamma(\alpha)k!(n-2k)!} \cdot \frac{a^{n+4}}{r^{n+2\alpha}} \cdot \mathbf{K}_1(n+1-2k) \cdot (2\mathbf{K}_2(n+2) - \mathbf{K}_2(n+4)) \quad (88)$$

There remain another two types of integrals related to the ϕ -component of the scattered electric field. Specifically, the $\mathbf{I}_{\phi}^{(1)}$ integral becomes

$$\mathbf{I}_{\phi}^{(1,1)} = \frac{4jk}{3\pi} k_{xi}^2 \cos\psi_i \sin\phi \mathbb{S}_8 \quad (89)$$

$$\mathbf{I}_{\phi}^{(1,2)} = -\frac{8jk}{3\pi} \cos\psi_i \sin\phi \mathbb{S}_8 \quad (90)$$

$$\mathbf{I}_{\phi}^{(1,3)} = \frac{8jk}{3\pi} k_{zi} \sin\psi_i \cos\phi \mathbb{S}_8 \quad (91)$$

where

$$\mathbb{S}_8 = \sum_{n=0}^{\infty} \sum_{k=0}^{\lfloor n/2 \rfloor} (-1)^k \frac{\Gamma(n-k+\alpha)(2\sin\theta)^{n-2k}}{\Gamma(\alpha)k!(n-2k)!} \cdot \frac{a^{n+3}}{r^{n+2\alpha}} \cdot \mathbf{K}_1(n-2k+2) \cdot (\mathbf{K}_2(n+1) - \mathbf{K}_2(n+3)) \quad (92)$$

Similarly, the $\mathbf{I}_{\phi}^{(2)}$ integral can be written as follows:

$$\mathbf{I}_{\phi}^{(2,1)} = 0 \quad (93)$$

$$\mathbf{I}_{\phi}^{(2,2)} = \frac{4jk}{3\pi} k_{xi}^2 \cos\psi_i \sin\phi \mathbb{S}_9 \quad (94)$$

$$\mathbf{I}_{\phi}^{(2,3)} = -\frac{4jk}{3\pi} \cos\psi_i \sin\phi \mathbb{S}_{10} \quad (95)$$

$$\mathbf{I}_{\phi}^{(2,4)} = \frac{4jk}{3\pi} k_{zi} \sin\psi_i \cos\phi \mathbb{S}_{10} \quad (96)$$

where

$$\mathbb{S}_9 = \sum_{n=0}^{\infty} \sum_{k=0}^{\lfloor n/2 \rfloor} (-1)^k \frac{\Gamma(n-k+\alpha)(2\sin\theta)^{n-2k}}{\Gamma(\alpha)k!(n-2k)!} \cdot \frac{a^{n+3}}{r^{n+2\alpha}} \cdot (\mathbf{K}_1(n-2k) - \mathbf{K}_1(n-2k+2)) \cdot (\mathbf{K}_2(n+1) - 2\mathbf{K}_2(n+3)) \quad (97)$$

$$\mathbb{S}_{10} = \sum_{n=0}^{\infty} \sum_{k=0}^{\lfloor n/2 \rfloor} (-1)^k \frac{\Gamma(n-k+\alpha)(2\sin\theta)^{n-2k}}{\Gamma(\alpha)k!(n-2k)!} \cdot \frac{a^{n+3}}{r^{n+2\alpha}} \cdot (\mathbf{K}_1(n-2k) - \mathbf{K}_1(n-2k+2)) \cdot (2\mathbf{K}_2(n+1) - \mathbf{K}_2(n+3)) \quad (98)$$

All the aforementioned results correspond to closed-form expressions derived using an exact analytical approach. A numerical evaluation of the field integrals results in computational errors which may be significant unless the discretization size becomes extremely small. Such an approach though requires computationally intensive codes, which often take enormous computer time to provide accurate and reliable results.

On the other hand, using the proposed analytical approach, highly accurate results of the scattered fields can be produced in a computationally efficient way. Analytical methods also provide insight and understanding into the scattering mechanisms of the geometry in hand and the overall wave behavior in the vicinity of the aperture.

3. NUMERICAL RESULTS

The validity and accuracy of the analytical method presented in the previous section was tested against a numerical integration approach based on Riemann sum. The numerical integration was applied directly on the double integrals shown in Eqs. (11)–(13) implementing fine differential lengths in order to ensure a high degree of accuracy at the expense of poor computational efficiency. For sufficient accuracy in the calculation of the scattered fields, the number of subdivisions in the ρ and ϕ directions must be 2000 and 2160, respectively. The corresponding CPU time on a PC with Intel processor i5-4460, 3.2 GHz and 16 GB RAM is 70 seconds per point.

For the first experiment, a linearly-polarized TM-wave ($\psi_i = 0^\circ$) was incident on the aperture at an angle 30 degrees from the vertical (see Fig. 2). The radius of the aperture is 0.316λ , where λ is the wavelength of the wave. The observation point resides along the radial direction defined by an elevation angle $\theta = 70^\circ$ and an azimuth angle $\phi = 45^\circ$. The three components of the scattered electric field (magnitude) are plotted as a function of the radial distance in the interval $a < r \leq 100a$. The analytical results are compared favorably against the numerical-integration results. It is important to emphasize here that the radial component of the scattered electric field decays much faster than the other two

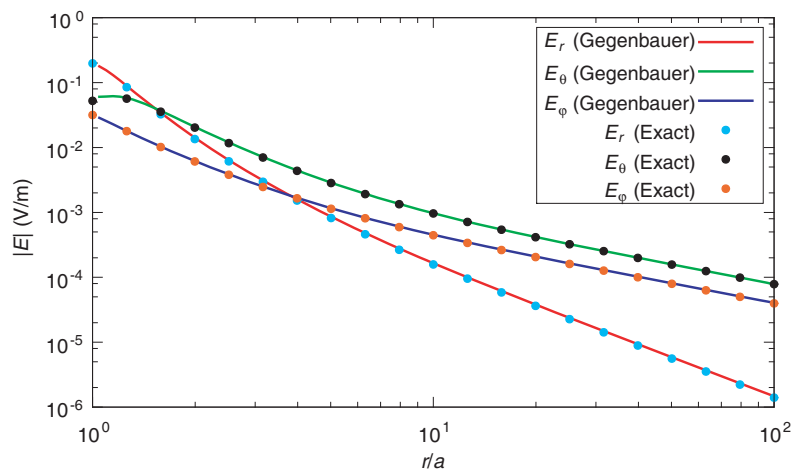


Figure 2. Magnitude of the scattered field components as a function of normalized observation distance: $\psi_i = 0$ (TM polarization), $\theta_i = 30^\circ$, $\phi_i = 0^\circ$, $\theta = 70^\circ$, $\phi = 45^\circ$.

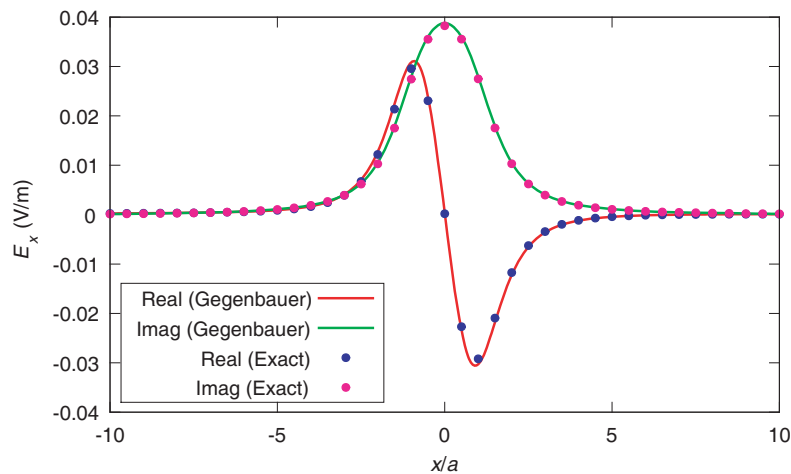


Figure 3. Real and imaginary parts of the x -directed scattered electric field along a line parallel to the x -axis defined by $z = 1.2a$: $\psi_i = 0$ (TM polarization), $\theta_i = 30^\circ$, $\phi_i = 0^\circ$.

components when the observation point moves farther away from the center of the aperture. This is expected as the radial component becomes negligible in the far-field region of observation. It is also worth mentioning at this point that the analytical results are produced based on 30 Gegenbauer terms and 70 Taylor-series expansion terms. The corresponding CPU time is 0.45 seconds per point, which is more than 150 times faster than the numerical approach based on Riemann sum.

A second experiment was conducted where the observation point moves along a parallel-to-the x -axis line defined by $z = 1.2a$. The polarization of the wave and the incident elevation angle remain the same as before. By maintaining the number of Gegenbauer and Taylor-series terms the same as in the previous experiment, the x and z components of the scattered electric field (real and imaginary) are illustrated in Figs. 3 and 4, respectively. A comparison between the analytical method and the numerical-integration approach is illustrated. As observed, the two sets of data compare favorably for the entire range of points; i.e., $-10a \leq x \leq 10a$. It is therefore evident that the analytical expressions derived in the previous section provide an accurate and computationally efficient approach for the quick computation of the scattered fields by a subwavelength aperture in a conducting screen.

Additional computational tests were conducted in order to evaluate the convergence of the Taylor-series expansion implemented in the underlined analytical approach. The magnitude of the θ -component

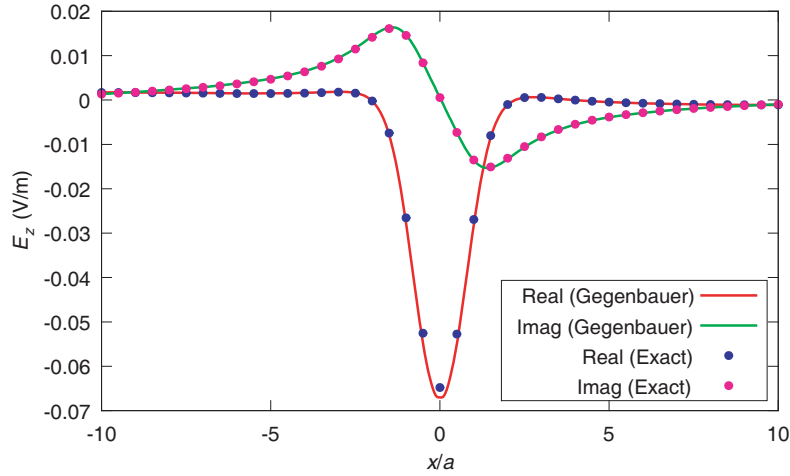


Figure 4. Real and imaginary parts of the z -directed scattered electric field along a line parallel to the x -axis defined by $z = 1.2a$: $\psi_i = 0$ (TM polarization), $\theta_i = 30^\circ$, $\phi_i = 0^\circ$.

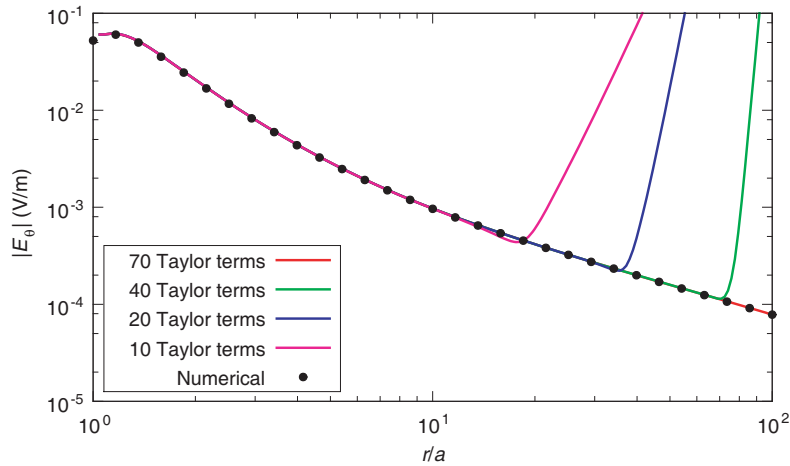


Figure 5. Taylor series convergence for the E_θ component as a function of the normalized radial distance: $\psi_i = 0$ (TM polarization), $\theta_i = 30^\circ$, $\phi_i = 0^\circ$, $\theta = 70^\circ$, $\phi = 45^\circ$.

of the electric field, as a function of the normalized radial distance, is plotted for different number of Taylor expansion terms in Fig. 5. As illustrated, by increasing the number of Taylor expansion terms, the analytical results converge to the numerical data. For example, if only 10 Taylor expansion terms are used, the accuracy is guaranteed up to a normalized radial distance equal to approximately 10. For accurate results in the entire range illustrated in the figure, it is important that at least 70 Taylor expansion terms are used. Note, however, that the Taylor series expansion becomes increasingly slower to converge as the number of terms rise. This is well understood as the Taylor-expansion point corresponds the origin of the coordinate system, which coincides with the center of the aperture.

Another important numerical test was performed regarding the convergence of the Gegenbauer polynomial expansion for the evaluation of the scattered field. The real and imaginary parts of the E_z component are shown plotted in Fig. 6 for a finite number of Gegenbauer terms. Specifically, we used 1, 2 and 5 Gegenbauer terms in the expansion of the scattered fields. It is clearly illustrated in this figure that a small number of Gegenbauer terms is sufficient to provide an accurate calculation of the scattered fields along a line parallel to the x -axis. The effect of adding more Gegenbauer terms in the expansion is more profound close to the axis of the aperture where the field is relatively stronger. As illustrated, the analytical results compare well with the numerical set of data, thus reinforcing the validity of the underlined analytical approach. Similar observations were noticed for all the components of the scattered field.

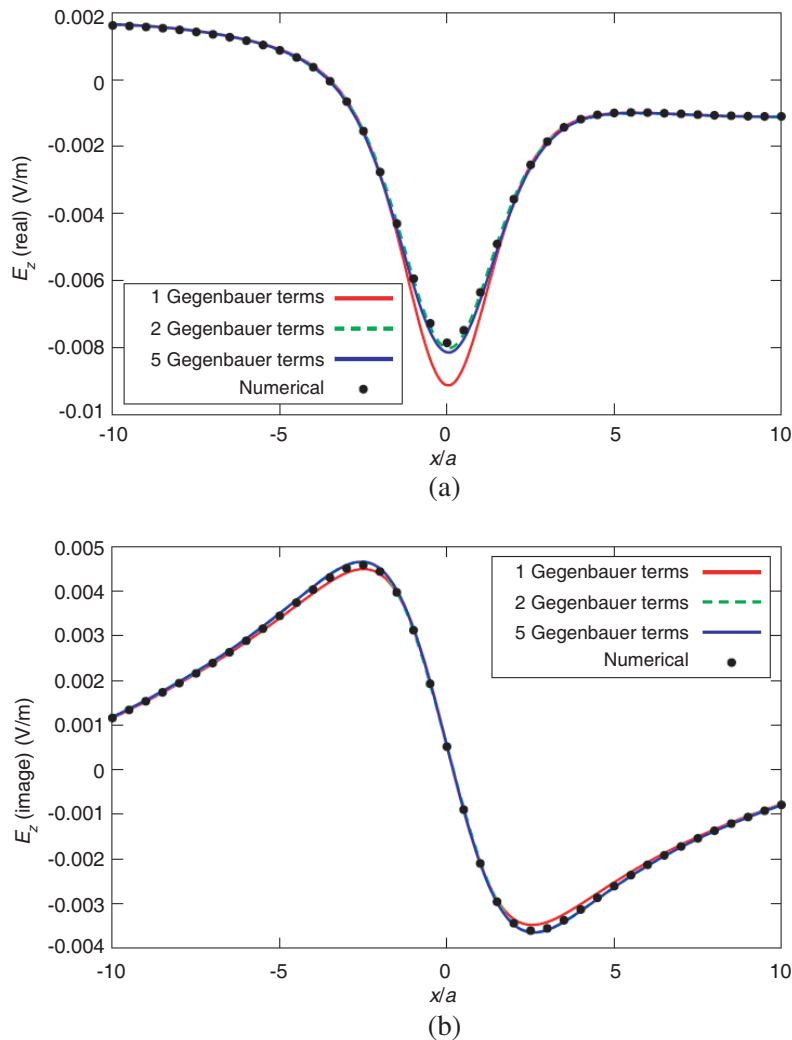


Figure 6. Gegenbauer series convergence: (a) Real E_z component; (b) Imaginary E_z component; Specifications: $z = 3a$, $\psi_i = 0$ (TM polarization), $\theta_i = 30^\circ$, $\phi_i = 0^\circ$.

4. CONCLUSIONS

In this paper, it was demonstrated that the scattered fields by a subwavelength circular aperture in an infinite conducting screen can be derived analytically for any observation point in the lower half plane. The underlined formulation, based on a Taylor-series expansion of the free-space Green's function and a judicious implementation of a Gegenbauer polynomial expansion for terms of the form $1/R^{2\alpha}$, resulted in closed-form expressions for the scattered electric fields by the aperture. Both expansions were highly convergent resulting in a computationally efficient algorithm for the calculation of the scattered fields in the near-, intermediate- and far-field regions of the aperture. The accuracy of the closed-form field expressions was illustrated for different scattering cases by comparing the analytical results with data obtained through a direct numerical integration of the governing radiation integrals. The underlined formulation is valid for any arbitrary observation point; however, as the observation distance extends to the far-field region of the aperture, the rate of convergence of the Taylor-series expansion increasingly slows down, deeming the approach less efficient.

REFERENCES

1. Mertz, J., *Introduction to Optical Microscopy*, Roberts and Company Publishers, United States of America, 2009.
2. Van Labeke, D. and D. Barchiesi, "Probes for scanning tunneling optical microscopy: A theoretical comparison," *Journal of Optical Society of America A*, Vol. 10, No. 10, 2193–2201, 1993.
3. Thio, T., K. M. Pellerin, R. A. Linke, H. J. Lezec, and T. W. Ebbesen, "Enhanced light transmission through a single subwavelength aperture," *Optics Letters*, Vol. 26, No. 24, 1972–1974, 2001.
4. Bethe, H. A., "Theory of diffraction by small holes," *Phys. Rev.*, Vol. 66, No. 10, 163–182, 1944.
5. Bouwkamp, C. J., "On Bethe's theory of diffraction by small holes," *Philips Res. Rep.*, Vol. 5, No. 10, 321–332, 1950.
6. Bouwkamp, C. J., "Diffraction theory. A critique of some recent developments," Washington Sq. College of Arts and Science, New York University, 1953.
7. Balanis, A. C., *Advanced Engineering Electromagnetics*, 2nd edition, Wiley, New Jersey, 2012.
8. Leviatan, Y., "Study of near-zone fields of a small aperture," *Journal of Applied Physics*, Vol. 60, No. 5, 1577–1583, 1986.
9. Nakano, T. and S. Kawata, "Numerical analysis of the near-field diffraction pattern of a small aperture," *Journal of Modern Optics*, Vol. 39, No. 3, 645–661, 1992.
10. Dürig, U., D. W. Pohl, and F. Rohner, "Near-field optical-scanning microscopy," *Journal of Applied Physics*, Vol. 59, No. 10, 3318–3327, 1986.
11. Miexner, J. and W. Andrejewski, "Strenge theorie der beugungebener elektromagnetischer wellen an der vollkommen leitenden kreisscheibe und an der kreisformigen Öffnung im vollkommen leitenden ebenen schirm," *Ann. Physik*, Vol. 7, 157–158, 1950.
12. Born, M. and E. Wolf, *Principles of Optics*, Pergamon Press, London, 1959.
13. Flammer, C., "The vector wave function of the diffraction of electromagnetic waves by circular disks and apertures. I. Oblate spheroidal vector wave functions," *Journal of Applied Physics*, Vol. 24, 1218–1223, 1953.
14. Roberts, A., "Electromagnetic theory of diffraction by a circular aperture in a thick, perfectly conducting screen," *Journal of Optical Society of America A*, Vol. 4, 197–198, 1987.
15. Van Labeke, D., D. Barchiesi, and F. Baida, "Optical characterization of nanosources used in scanning near-field optical microscopy," *Journal of Optical Society of America A*, Vol. 12, No. 4, 695–703, 1995.
16. Van Labeke, D., F. Baida, D. Barchiesi, and D. Courjon, "A theoretical model for the inverse scanning tunneling optical microscope (ISTOM)," *Opt. Commun.*, Vol. 114, Nos. 5–6, 470–480, 1995.

17. Michalski, K. A., "Spectral domain analysis of a circular nano-aperture illuminating a planar layered sample," *Progress In Electromagnetics Research B*, Vol. 28, 307–323, 2011.
18. Michalski, K. A., "Complex image method analysis of a plane wave-excited subwavelength circular aperture in a planar screen," *Progress In Electromagnetics Research B*, Vol. 27, 253–272, 2011.
19. Kobayashi, I., "Darstellung eines potentials in zylindrischen koordinaten, das sich auf einer ebene unterwirft," *Science Reports of the Thohoku Imperifal Unversity*, Ser. I, Vol. XX, No. 2, 197–212, 1931.
20. Nomura, Y. and S. Katsura, "Diffraction of electric wave by circular plate and circular hole," *Sci. Rep., Inst., Electr. Comm.*, Vol. 10, 1–26, Tohoku University, 1958.
21. Hongo, K. and Q. A. Naqvi, "Diffraction of electromagnetic wave by disk and circular hole in a perfectly conducting plane," *Progress In Electromagnetic Research*, Vol. 68, 113–150, 2007.
22. Michalski, K. A. and J. R. Mosig, "On the plane wave-excited subwavelength circular aperture in a thin perfectly conducting flat screen," *IEEE Trans. Antennas Propag.*, Vol. 62, 2121–2129, 2014.
23. Michalski, K. A. and J. R. Mosig, "Analysis of a plane wave-excited subwavelength circular aperture in a planar conducting screen illuminating a multilayer uniaxial sample," *IEEE Trans. Antennas Propag.*, Vol. 63, 2054–2063, 2015.
24. Polycarpou, A. C. and A. M. Christou, "Closed-form expressions for the on-axis scattered fields by a sub-wavelength circular aperture in an infinite conducting plane," *IEEE Trans. Antennas Propag.*, Vol. 65, 978–982, 2017.
25. Arfken, G. B. and H. J. Weber, *Mathematical Methods for Physicists*, 6th edition, Elsevier, 2005.